Annals of Biomedical Engineering, Vol. 49, No. 12, December 2021 *(© 2021)* pp. 3374–3387
https://doi.org/10.1007/s10439-021-02828-6

Virtual Physiological Human

Parametric Analysis of an Integrated Model of Cardio-respiratory Interactions in Adults in the Context of Obstructive Sleep Apnea

GUSTAVO GUERRERO, VIRGINIE LE ROLLE, and ALFREDO HERNÁNDEZ

Univ Rennes, Inserm, LTSI - UMR 1099, Campus de Beaulieu, Bât 22, 35042 Rennes, France

(Received 8 February 2021; accepted 20 June 2021; published online 31 August 2021)

Associate Editor Stefan Duma oversaw the review of this article.

Abstract—An original integrated model of cardio-respiratory interactions is presented in this paper with the objective of studying the acute physiological responses evoked by obstructive sleep apnea events in adults. A comprehensive sensitivity analysis of the model is proposed during the simulation of a 20 s obstructive apnea episode using the Morris' screening method and local sensitivity analysis. The more relevant parameters are related to the following mechanisms of the physiology: (i) the fraction of oxygen in inspired air, (ii) metabolic rates (oxygen consumption rate, CO_2 production rate); (iii) chemoreflex (gains and time constants) (iv) respiratory mechanics (lung compliance and unstressed volume of air in the alveoli). These results highlight significant physiological variables that may be particularly useful for the development of novel diagnostic and therapeutic strategies, integrating a virtual patient approach.

Keywords—Cardiorespiratory model, Sensitivity analysis, *In silico*, Sleep disorders.

INTRODUCTION

Obstructive sleep apnea (OSA) is a multifactorial condition characterized by episodic sleep state-dependent collapse of the upper airway, resulting in periodic reductions or cessations in ventilation[10] lasting more than 10 seconds. These events cause acute cardio-respiratory responses (oxygen desaturation, intermittent hypoxia, sudden autonomic responses) and significant changes in sleep patterns.[19] In the long term, these acute effects increase the possibility of suffering from various chronic pathologies, such as high blood pressure, stroke, heart failure, and certain metabolic disorders.[39] It is estimated that between 6 and 17% of the adult population suffers from OSA, which represents a major public health problem.[36] However, the physiological mechanisms of OSA are still not fully elucidated. The interpretation of acute cardio-respiratory responses to apnea and hypopnea can be difficult, due to the variety of processes involved (autonomic regulation, cardiovascular, respiratory, chemoreflex, *etc.*), which must be jointly considered for a proper analysis. In this context, a model-based approach seems particularly adapted, as it allows the explicit integration of physiological knowledge into a data processing chain, as well as the analysis of the underlying mechanisms that are often difficult to observe.

Most of the models proposed in the literature represent isolated aspects of physiology, and only a limited number are integrated cardio-respiratory models. However, these models either lack certain mechanisms relevant to the dynamics of apneas[5,11,41] or are too complex to be used for a patient-specific analysis.[3,9] For these reasons, to our knowledge, no comprehensive model of cardio-respiratory interactions has been used to analyze acute cardio-respiratory responses of adult apneas. Our team has also proposed several integrated models of the respiratory[2,31] and the cardiovascular systems.[6,7,34] The first objective of this work is thus to propose an original ordinary differential equation (ODE) integrated model of cardio-respiratory interactions, useful for the analysis of acute cardio-respiratory responses to apnea. The proposed model is a further development of a preliminary integrated model recently presented by our group,[13] in which we have improved the representation of cardio-

Address correspondence to Virginie Le Rolle, Univ Rennes, Inserm, LTSI - UMR 1099, Campus de Beaulieu, Bât 22, 35042 Rennes, France. Electronic mail: virginie.lerolle@univ-rennes1.fr

respiratory interactions and gas exchange as well as introduced a pulmonary shunt in the circulation.

Once an appropriate model is available, sensitivity analysis methods appear as useful tools to cope with the complexity of physiological systems. These methods provide insights into the relations between model parameters and model outputs and allow for quantitative characterization of the relative significance of each parameter.[18] Determination of the most sensitive parameters provides key information towards patient-specific modeling and is an essential step to better understand the underlying physiological mechanisms within complex systems. The second objective of this paper is thus to analyze the effects of the most relevant parameters of the proposed model during the simulation of an obstructive apneic event, by applying a set of sensitivity analysis methods.

The paper is organized as follows: In "Materials and Methods" section, the computational model is described and the sensitivity analysis method is explained. In "Results" section , the results of applying the described methods are presented. Discussion and conclusions are finally specified in "Discussion" section.

MATERIALS AND METHODS

Integrated Cardio-respiratory Model

Figure 1 shows the global structure of the proposed model that is composed of four interconnected components: (i) the respiratory system, (ii) the cardiovascular system, (iii) the gas exchange (in the lungs and the metabolism) and (iv) the neural control. The integrated model includes 42 state variables and 151 parameters and was implemented using the "Multi-formalism Modelling and Simulation Library" (M2SL).[16] This library, which is developed and maintained by our team, is based on the co-simulation principle and has been applied for modeling and simulation on cardiovascular, respiratory and renal physiopathology in a number of scientific papers. M2SL is a collection of generic C++ classes that has been specifically developed for modelling and simulating complex systems using a combination of different modelling formalisms. Access to M2SL source code can be granted by contacting the authors.[16]

Equations, parameters, and verification of model simulations and outputs with reference values from the literature can be found in the supplementary online material.

Cardiovascular System (CVS) Model

The CVS model (Fig. 2) is an adaptation of previous models of our group.[8,34] This representation is composed of (a) the cardiac electrical system, (b) cardiac cavities, and (c) systemic and pulmonary circulations. The model simulates pulsatile blood pressure, volumes, and flows, as shown of figure 3.1 of supplementary materials.

Cardiac Electrical System

The electrical conduction system is defined as a set of coupled cellular automata adapted from Hernández *et al.*[15] Each interconnected automaton represents the electrical activation of a group of cardiac cells: the sinoatrial node, the left atrium (LA), the atrioventricular node, the upper bundle of His, the lower bundle of His, left and right bundle branches, and left and right ventricles (LV and RV). The output electrical activations of LV and LA trigger the mechanical contractions of the ventricles and the atrium chambers of the CVS model respectively.

Elastance-Based Cardiac Cavities

The pressure of each cardiac cavity is represented by a combination of end-systolic and end-diastolic pressure-volume relationships, driven by time-varying elastances:

(i) a Two-hill driving function for RV and LV,[27] and (ii) a gaussian function[26] for the atria. Volume (V) in each cavity is calculated from the integral of their respective net flow (ΔQ). The heart valves (mitral, aortic, tricuspid, and pulmonary) are represented as idealized diodes.

Systemic and Pulmonary Circulations

The arteries, veins, and capillaries of systemic and pulmonary circulations were included, as well as intrathoracic and extrathoracic compartments. Pressure (P) of each compartment is computed as a linear function between the elastance (E) and the blood volume (V). The thoracic pressure (P_{tor}) from the respiratory system is added to the pressure of every intrathoracic compartment. The blood flow (Q) circulating between two chambers is calculated by dividing the pressure gradient between the resistance between compartments $\left(Q = \frac{\Delta P}{R}\right)$.

Three compartments were added in the circulation model (Fig. 2), to integrate the gas exchange to the cardio-respiratory model following the structure of Albanese *et al.*[3] First, a chamber representing the systemic peripheral vessels was included in the systemic circulation to integrate the metabolic gas exchange

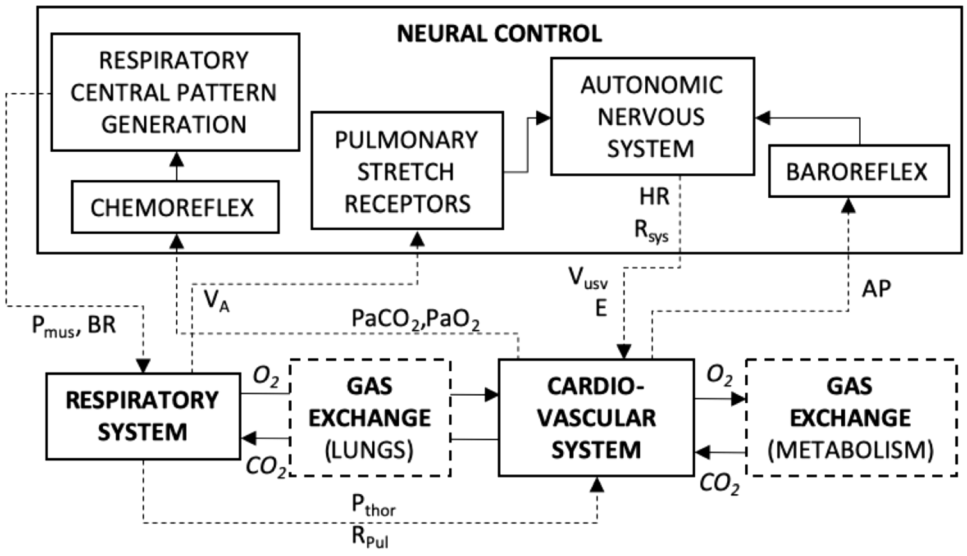

FIGURE 1. General diagram of the cardio-respiratory adult model. Dotted line arrows symbolize interactions between sub-models. P_{thor} thoracic pressure, R_{pul} pulmonary capillaries resistance, P_{mus} respiratory muscles pressure, *BR* breathing rate, V_A alveolar volume, PaO_2 *and* $PaCO_2$ partial pressure of O_2 and CO_2 in the systemic arteries, respectively, *HR* heart rate, R_{sys} systemic peripheral resistance, V_{usv} unstressed volume of the systemic veins, *E* ventricle elastances, *AP* arterial pressure.

sub-model. Second, two parallel chambers, including pulmonary peripheral vessels (blood passing through the pulmonary capillaries) and a pulmonary shunt (blood not involved in the lung gas exchange), were integrated into the pulmonary circulation to represent lung gas exchanges. Resistance (R_{ps}; R_{pp}) and compliance values (C_{ps}, C_{pp}) of these last two compartments were assigned to distribute the desired percentage of blood flow (fs) coming out of the pulmonary arteries to the pulmonary shunt, as presented in Eqs. 1 and 2.

$$R_{\mathrm{ps}} = R_{\mathrm{pp}} \cdot \frac{(1 - fs)}{fs} \tag{1}$$

$$R_{\mathrm{ps}} = R_{\mathrm{pp}} \cdot \frac{(1 - fs)}{fs} \tag{2}$$

Finally, the effect of lung inflation in the resistance of pulmonary capillaries was included in the following equation[22]:

$$R_{\mathrm{pa}}(V_{\mathrm{A}}) = R_{\mathrm{pa},0} \cdot \left(\frac{V_{\mathrm{A}}}{V_{\mathrm{A,max}}}\right)^2 \tag{3}$$

where R_{pa} is the resistance of pulmonary arteries, V_{A} is the alveolar volume, $R_{\mathrm{pa},0}$ is a constant to set the normal resistance value of the pulmonary arteries, and $V_{\mathrm{A,max}}$ the maximum alveolar volume.

Respiratory Model

The respiratory model (Fig. 3) is an adaptation of previous works of our team[33] and Avanzolini *et al.*[4] It represents the upper, intermediate, and lower airways, the dead space, the alveolar compartment, the pleural cavity, the chest wall, and the respiratory muscles.

The intermediate airway compartment, the chest wall, and the alveolar space are assumed to have a constant purely elastic behavior, represented respectively by constant compliances C_{c}, C_{cw} and C_{A} and unstressed volumes V_{uc}, V_{ucw} and V_{uA}.

Tracheobronchial airways resistances are characterized by nonlinear relationships.[4] The respiratory muscles pressure is defined by a function P_{mus} defined by Le Rolle *et al*[33]:

$$P_{\mathrm{mus}} = P_{\max} \cdot \left(B_0 + (1 - B_0) \cdot \left(\frac{t_r}{T_1}\right)^{\beta} \cdot e^{-\left(\left(\frac{t_r}{T_1}\right)^{\alpha} - 1\right)}\right) \tag{4}$$

here $P_{\max}$ corresponds to maximum muscle activity, B_0 is the basal level at end-expiration, t_{r} is the time elapsed from the onset of the current respiratory cycle, T_{I} is the inspiration duration, and α and β characterize the P_{mus} signal profile during inspiration and expiration, respectively. This function reproduces realistic respiratory pressure and flow profiles. $P_{\max}$ and the breathing rate of this sub-model are controlled by the chemoreflex model.

Gas Exchange Model

This sub-model is composed of three components: (a) lung gas exchange, (b) metabolism gas exchange and (c) gas transport.

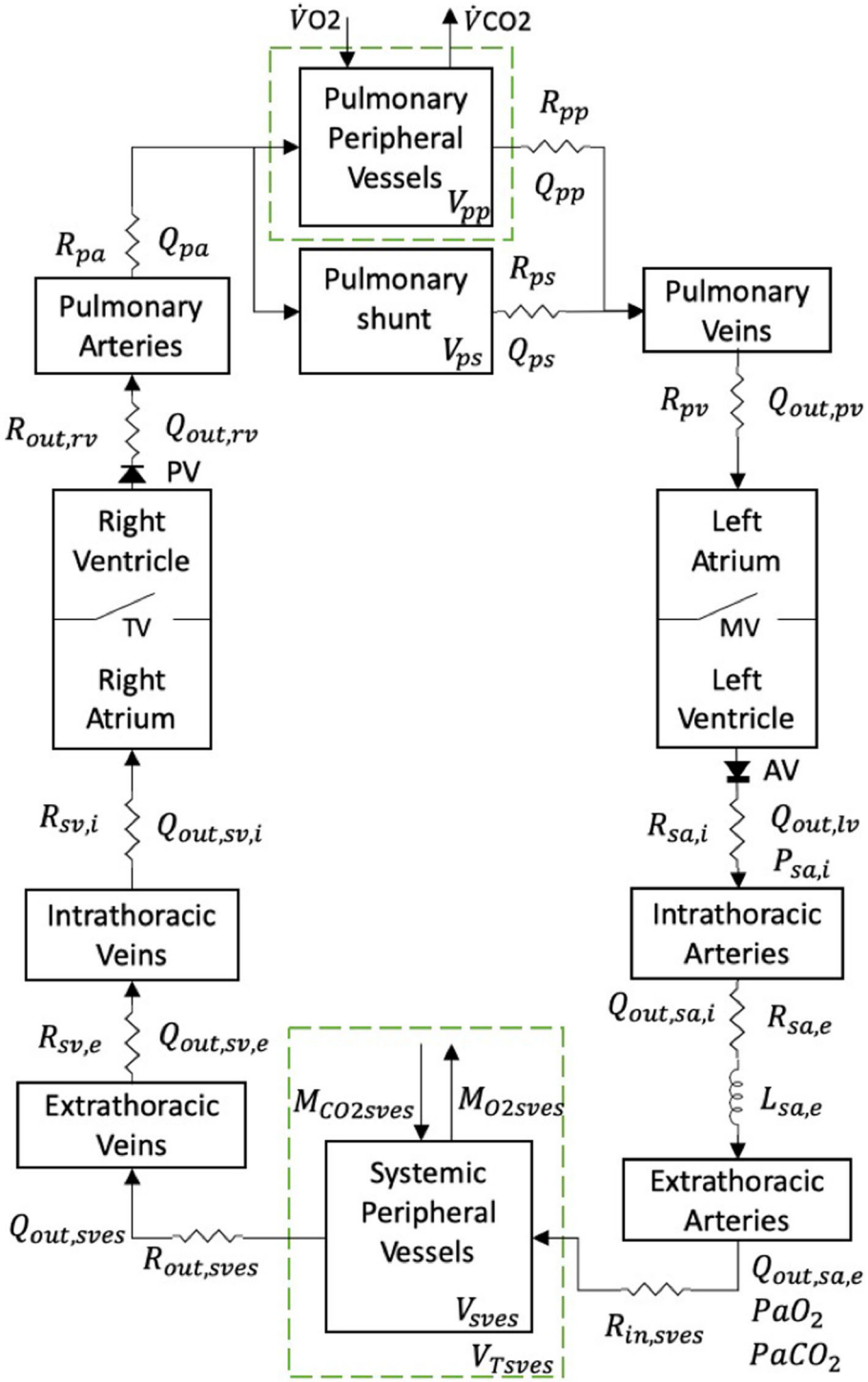

FIGURE 2. Diagram of the cardiovascular system model. Each compartment is characterized by an elastance (E) and its pressure (P) and volume (V) are computed. Green dotted line blocks correspond to the interface with the gas exchange sub-models. *Q* flow, *R* resistance, *L* inertia, *ra* right atrium, *rv* right ventricle, *la* left atrium, *lv* left ventricle, *tv* tricuspid valve, *mv* mitral valve, *pa* pulmonary arteries, *pp* pulmonary peripheral, *pv* pulmonary veins, *sa* systemic arteries, *sves* systemic peripheral vessels, *sv* systemic veins, *i* intra-thoracic, *e* extra-thoracic, *M* metabolic rates, *V* flow. The dotted-line compartments represent the gas exchange: *Top* Lung gas exchange in the pulmonary peripheral vessels; *Bottom* Metabolic gas exchange in the systemic peripheral vessels.

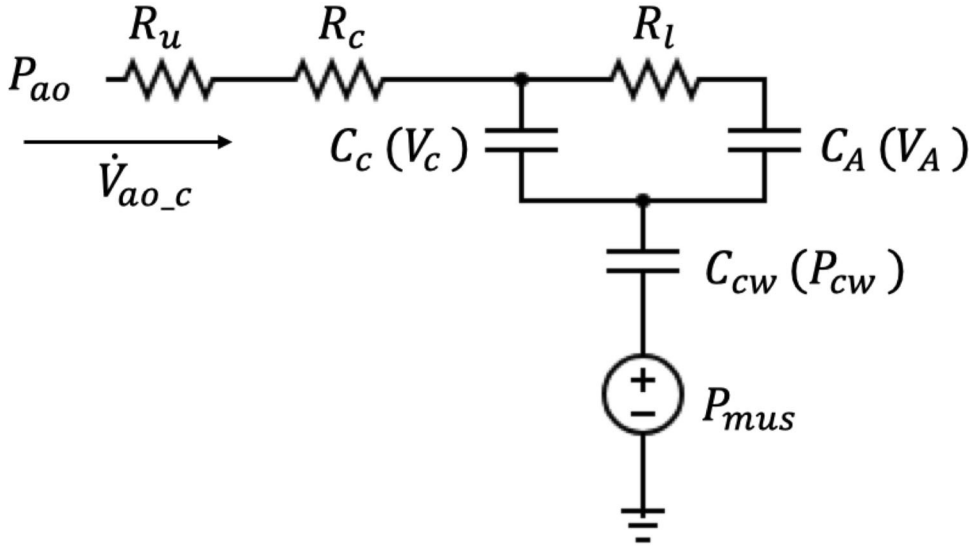

FIGURE 3. Electric diagram of the respiratory system model. *P* pressure, *R* resistance, *V* volume, *C* compliance, $\dot{V}$ airflow, *ao* airway opening, *u* upper airway, *c* intermediate airways, *l* lower airways, *pl* pleural, *cw* chest wall, *A* alveolar, *mus* respiratory muscles, $\dot{V}_{ao\_c}$ airflow from the airway opening to the lower airways, also denominated lung respiratory flow.

Lung Gas Exchange

The lung gas exchange model (Fig. 4) represents the exchange of O_2 and CO_2 between the pulmonary capillaries, the alveolar space, the dead space, and the inspired air. This model is an adaptation of Albanese *et al.*[3] and Ellwein *et al.*[11]

The sub-model has several inputs from other sub-models:

1. From the respiratory model: The dead volume, represented by the intermediate airway volume (V_c), the alveolar volume ($V_{\dot{A}}$) and flow V_A, and the lung respiratory flow V_l.
2. From the CVS model: the volume of blood in the pulmonary peripheral vessels (V_{pp}) and the blood flow through the pulmonary artery, peripheral circulation, and shunt (Q_{pa}, Q_{pp}, and Q_{ps}).
3. From the metabolic gas exchange and gas transport model: The delayed venous gas concentrations in the blood ($\tilde{C}_{v,CO_2}, \tilde{C}_{v,CO_2}$).

Fractions of inspired gases (FIO_2, $FICO_2$) are external inputs specific for this submodel. Conservation of mass is applied to calculate the fractions and partial pressures of each gas in each compartment, assuming that every compartment is homogeneous and perfectly mixed. The ideal gas law is used to obtain the fractions of gas from the partial pressure and vice-versa. Oxygen dissociation curves[38] are used to convert partial pressures to gas concentrations. These dissociation functions consider both the Haldane and the Bohr effects. An instantaneous equilibrium between pulmonary capillaries and alveoli gas partial pressures is assumed.

The outputs of the model are the blood gases concentrations in pulmonary capillaries ($C_{A,gas}$, gas $\in \{O_2, CO_2\}$). This oxygenated blood is then mixed with the blood that did not take part in the lung gas exchange in the pulmonary shunt, obtaining arterial blood gas concentrations ($C_{a,gas}$).

Metabolic Gas Exchange

This sub-model corresponds to the production of CO_2 and the consumption of O_2 by the systemic tissues and organs. This representation was adapted from Albanese *et al.*[3] and integrated into the systemic peripheral vessels of the CVS sub-model (Fig. 2). This blood-tissue compartment is modeled as a simple container with a total volume given by the sum of the constant tissue volume ($V_{T,sves}$) and the blood volume of the systemic peripheral vessels V_{sves}. The metabolic rates are assumed as constants, M_{O2sves} for the O_2 and $M_{CO2sves}$ for the CO_2. The inputs of this sub-model are the delayed arterial gas concentrations from the lung gas exchange model after the gas transport ($\tilde{C}_{O_2}, \tilde{C}_{CO_2}$), and the volume ($V_{sves}$) and the blood flows ($Q_{out,sa,e}$) of the systemic peripheral vessels from the CVS.

The conservation of mass principle is used in the systemic tissue to obtain the output gas concentration in the mixed venous blood (C_{svesO2}, $C_{svesCO2}$) as shown by Eqs. 5 and 6:

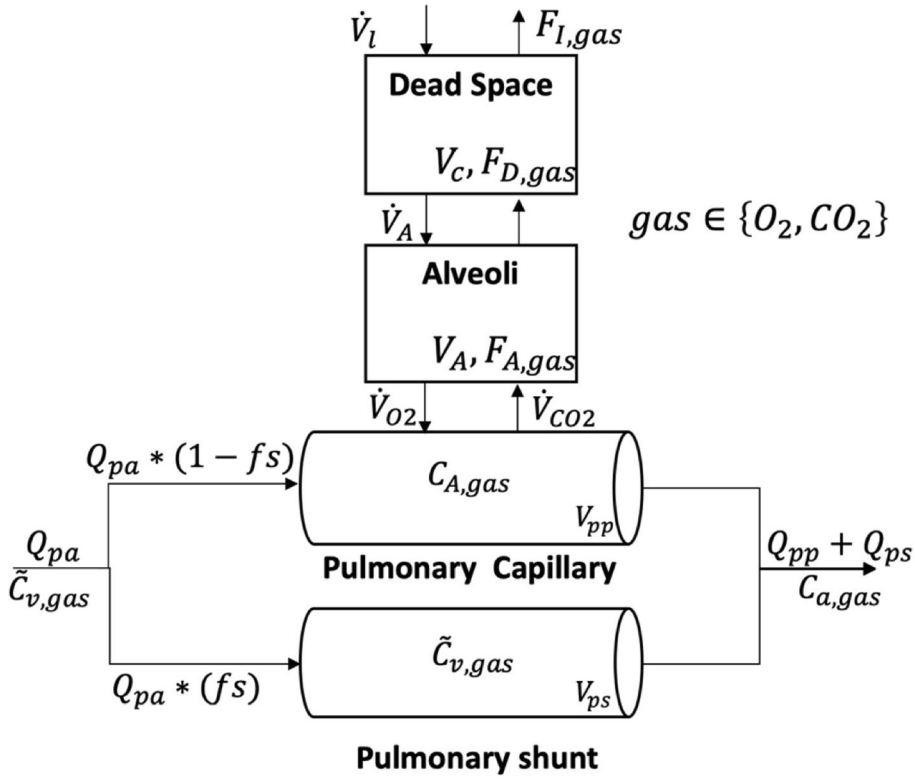

FIGURE 4. Lung gas exchange model. *F* gas fraction, *V* volume, *Q* blood flow, *C* concentration, *I* inspired, *D* dead space, *A* alveolar, *a* arterial, *v* venous, *out,pa* pulmonary capillaries, *fs* shunt fraction, *l* lung.

$$(V_{\mathrm{T,sves}} + V_{\mathrm{sves}}) \cdot \frac{\mathrm{d}c_{\mathrm{svesO2}}}{\mathrm{d}t} = Q_{\mathrm{out,sa},e} \cdot (\tilde{C}_{\mathrm{a,O2}} - C_{\mathrm{svesO2}}) - M_{\mathrm{O2sves}} \tag{5}$$

$$(V_{\mathrm{T,sves}} + V_{\mathrm{sves}}) \cdot \frac{\mathrm{d}c_{\mathrm{svesCO2}}}{\mathrm{d}t} = Q_{\mathrm{out,sa},e} \cdot (\tilde{C}_{\mathrm{a,CO2}} - C_{\mathrm{svesCO2}}) - M_{\mathrm{CO2sves}} \tag{6}$$

Gas Transport

This sub-model describes the transport of O_2 and CO_2 throughout the CVS. Pure delays τ_{LT} and τ_{VL} are used to represent the time that blood takes to transport the gases from the pulmonary capillaries to the systemic peripheral vessels and from the extra-thoracic veins to the pulmonary capillaries, respectively. τ_{LT} represents the time that takes for the blood to travel from the lung to the pulse oximeter sensor site.[28] Moreover, the conservation of mass principle is applied to every vein compartment to explicitly represent the transport throughout the intra-thoracic and extra-thoracic veins.

Neural Control

Chemoreflex Model

The chemosensory feedback was included in the integrated model using the peripheral and central chemoreflex sub-models (Fig. 5a), adapted from Albanese *et al.*[3] These sub-models modulate the breathing rhythm (BR) and the respiratory muscle maximal amplitude (P_{max}) in response to changes of PaO_2 and $PaCO_2$. The central chemoreflex is described as a first-order system characterized by time constants ($\tau_{\mathrm{c,f}}$, $\tau_{\mathrm{c,A}}$) and specific gains ($G_{\mathrm{c,A}}$, $G_{\mathrm{c,f}}$) and with a pure delay (D_{c}). The central chemoreceptors are assumed to be sensitive to the variations of $PaCO_2$ concerning a set-point value $PaCO_{2,n}$. On the other hand, the peripheral chemoreflex is described as a two-stage transduction mechanism. PaO_2 and $PaCO_2$ are first transduced into the afferent electrical activity of the peripheral chemoreceptors (f_{acp})[42] and then filtered by a set of first-order systems, defined by gains ($G_{\mathrm{p,A}}$, $G_{\mathrm{p,f}}$) and time constants ($\tau_{\mathrm{p,f}}$, $\tau_{\mathrm{p,A}}$), and by a pure delay (D_{p}).

Moreover, the maximum pressure of the respiratory muscles (P_{max}) and the breathing rhythm (BR) are computed by summing the contributions of each chemoreceptor (ΔP_{maxc}, ΔP_{maxp}, ΔBR_{c} and ΔBR_{p}) to the baseline response of each regulated variable.

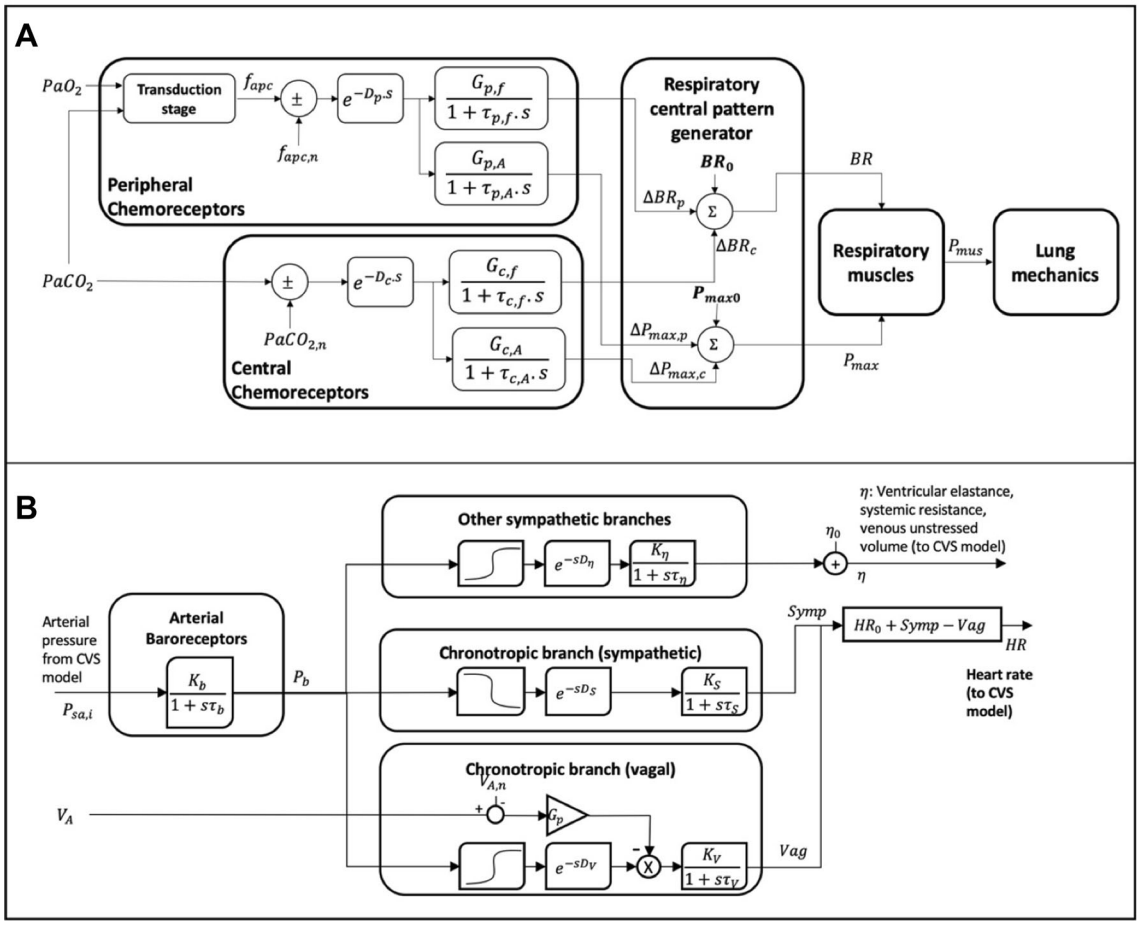

FIGURE 5. Neural control sub-models. a Chemoreflex model. *Pa* arterial partial pressure, *D* delay, *BR* breathing rhythm, P_{mus} activity of respiratory muscles, P_{max} maximum amplitude of the activity of respiratory muscles, f_{apc} afferent electrical activity of the peripheral chemoreceptors, *c* central chemoreflex, *p* peripheral chemoreflex, *A* amplitude, *f* frequency. b Baroreflex model. From the arterial pressure registered at the intrathoracic systemic circulation, the baroreflex system regulates the heart rate, the systemic resistance, the venous unstressed volume and the ventricular elastance. *K* gain, *D* delay, τ time constant, *G* gain, V_A lung volume.

These contributions are calculated following Eqs. 7 and 8:

$$\frac{\mathrm{d}\Delta P_{\max i}}{\mathrm{d}t} = \frac{-\Delta P_{\max i} + G_{i\mathrm{A}\cdot u_i}}{t_{i,\mathrm{A}}} \tag{7}$$

$$\frac{\mathrm{d}\Delta BR_i}{\mathrm{d}t} = \frac{-\Delta BR_i + G_{i,f\cdot u_i}}{t_{i,f}} \tag{8}$$

where $i \in \{p, c\}$ with p and c corresponding respectively to peripheral and central 10 chemoreceptors; u is the difference of the chemoreflex activity compared to its 11 reference value.

Baroreflex and Pulmonary Stretch Receptors

Baroreflex model (Fig. 5b) is adapted from previous work of our laboratory.[32,34] The afferent pathways of the arterial baroreceptors are represented by a first-order transferfunction (gain K_b and time constant T_b). Efferent sympathetic and vagal pathways are represented by a combination of sigmoid functions, delays (D_S and D_V respectively) and first-order filters, characterized by gains (K_S, K_V) and time constants (T_S, T_V).

Chronotropic control is represented as a combination of the contributions of sympathetic and parasympathetic branches. Systemic resistance, venous volume, and ventricular elastances are only influenced by the sympathetic system. The pulmonary stretch receptors modulate the vagal branch of the baroreflex in relation to the changes of lung volume V_A[30]. This is one of the main generators of the respiratory sinus arrhythmia (RSA),[29] a fluctuation of heart rate in phase with inspiration and expiration, with heart rate increasing during inspiration and decreasing during exhalation.

Sensitivity Analysis

A sensitivity analysis through the Morris' screening method[24] was performed to determine the most influential parameters of the model during and after an obstructive apnea event. This method was chosen because of its ability to provide a global rank of importance among parameters while preserving computational costs. The Morris' screening method consists in generating several random trajectories through the parameter space. Each trajectory is associated with an estimation of the Elementary Effects EE_i, defined for a parameter x_i:

$$EE_i = \frac{|F(x_1, ..., x_i, ...x_k) - F(x_1, ...x_i + \Delta, ...x_k)|}{\Delta} \quad (9)$$

where F is a function of the model output variables, $(x_1, \ldots, x_j, \ldots, x_k)$ is randomly selected point, $\Delta = \frac{p}{2(p-1)}$ is the perturbation applied to the parameter x_i, and p is defined as the number of levels that divide the parameter space. EE_i are calculated r times and the mean μ_i and standard deviation σ_i of these r realizations are then computed for each parameter i. Then, a sensitivity index D_{Mi} is calculated[6]:

$$D_{Mi} = \sqrt{(\mu_i)^2 + (\sigma_i)^2} \quad (10)$$

applied to all parameters x_i. This index provides a rank of the parameter effects; parameters with a high sensitivity will have a high D_{Mi}, while unimportant ones are associated with a low D_{Mi}.

Two output functions $F = \text{Delta}_X$ and $\text{Delta}^{\text{Mean}}{}_X$, with $X \in \{SaO_2, PaO_2, PaCO_2, HR\}$, were defined for our sensitivity analysis (Fig. 6):

(1) between the start and the end of an apnea event (Green circles in Fig. 6):

$$\text{Delta}_X = \frac{X_{\text{EndApnea}} - X_{\text{StartApnea}}}{X_{\text{StartApnea}}} \quad (11)$$

(2) computed over a support of 15 s window before the apnea and a 15 s window after the apnea (dashed rectangles in Fig. 6):

$$\text{Delta}_X^{\text{Mean}} = \frac{X_{\text{MeanAfter}} - X_{\text{MeanBefore}}}{X_{\text{MeanBefore}}} \quad (12)$$

The obstructive apnea event was simulated by increasing the resistance of the upper airways R_u of the respiratory model to 10,0000 $\text{cmH}_2\text{O} \cdot \text{s} \cdot \text{l}^{-1}$ at time $t = 30$ s to mimic a complete obstruction of the airways. The screening method was implemented in MATLAB, and was applied to all 151 parameters of the model. 60 realizations were calculated per parameter ($r = 60$), parameter ranges were selected from the nominal values ± 30%, and the parameter space was regularly divided as a grid of 16 levels ($p = 16$).

The most important parameters were selected using the following quantitative approached to perform a local sensitivity analysis:

(1) The indexes D_{Mi} calculated with the Morris screening method are normalized with respect to the total sum for each output function Delta_X and $\text{Delta}^{\text{Mean}}{}_X$ with $X \in \{SaO_2, PaO_2, PaCO_2, HR\}$.
(2) The median of the normalized $D_{Mi}'s$ is calculated per parameter for the 4 Delta_X and the 4 $\text{Delta}^{\text{Mean}}{}_X$.
(3) The medians are ranked and the parameters that comprise 70% of the normalized D_{Mi} are selected.

The local sensitivity analysis was performed to analyze the influence of these parameters on cardiorespiratory signals as the PaO_2, $PaCO_2$, SaO_2, and the heart rate.

RESULTS

Results of sensitivity analysis methods are separated into two sub-sections associated with the Morris' screening method and the local analysis.

Sensitivity Analysis Using the Morris's Screening Method

Figures 7a and 7b show the 6 most sensitive model parameters for each

Delta_X and $\text{Delta}^{\text{Mean}}{}_X$, during an obstructive apnea event. Metabolic rates (M_{O2sves} and $M_{CO2sves}$) and fraction of oxygen in inspired air (FIO_2) are part of the most influent parameters for Delta_{SaO2}, Delta_{PaO2}, Delta_{PaCO2}, $\text{Delta}^{\text{Mean}}{}_{SaO2}$, $\text{Delta}^{\text{Mean}}{}_{PaO2}$ and $\text{Delta}^{\text{Mean}}{}_{PaCO2}$. Concerning Delta_{SaO2}, Delta_{PaO2}, Delta_{PaCO2} and $\text{Delta}^{\text{Mean}}{}_{PaCO2}$, respiratory mechanics parameters (V_{uA}, C_A) also appear as important. The total volume in the systemic tissue ($V_{T,sves}$) is relevant for Delta_{SaO2} and Delta_{PaCO2}. The fraction of pulmonary shunt (fs) and the gain of the baroreceptors (K_b) are respectively significant for Delta_{PaO2} and Delta_{PaCO2}. Chemoreflex gains ($G_{c,A}$ and $G_{p,A}$) and the time constants ($\tau_{c,A}$ and $\tau_{p,A}$) of central and peripheral chemoreflex are highly influent on $\text{Delta}^{\text{Mean}}{}_{SaO2}$, $\text{Delta}^{\text{Mean}}{}_{PaO2}$ and $\text{Delta}^{\text{Mean}}{}_{PaCO2}$.

Concerning Delta_{HR}, no parameter stands out in the sensitivity analysis, because the heart rate does not change strongly in the model simulations during the

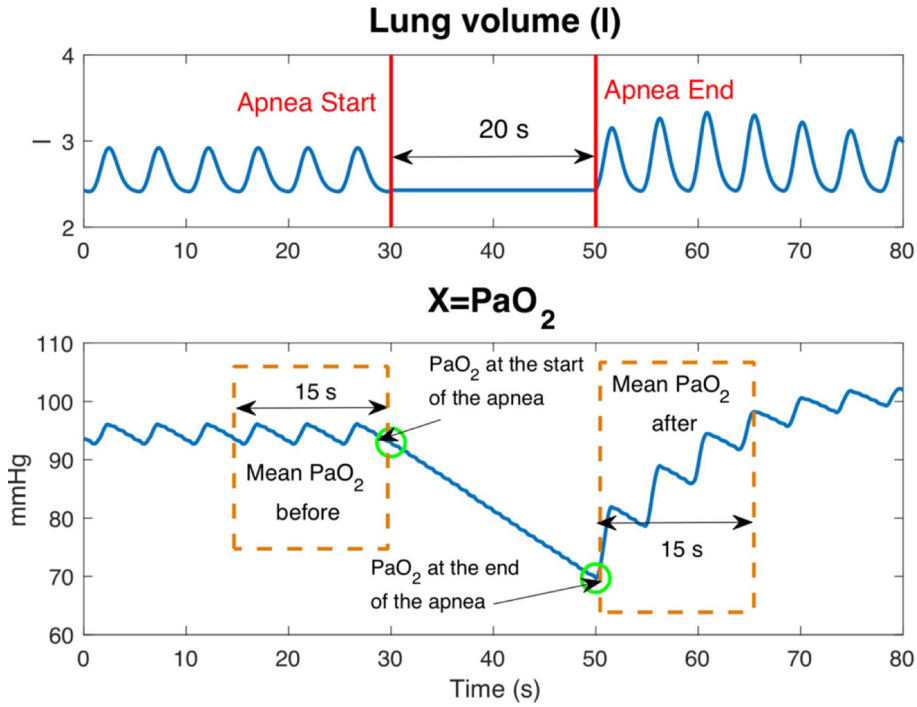

FIGURE 6. Example of a variable used in the sensitivity analysis (X) and how the Delta_X and $\text{Delta}^{\text{Mean}}{}_X$ markers are obtained from a simulation of a 20 s obstructive apnea. In this case, $X = \text{PaO}_2$, which is represented as simulated at the output of pulmonary capillaries. The green circles represent the values of X at the start and at the end of the apnea event. These values are used to calculate Delta_X. The orange dashed-line rectangle represents the 15 s window before and after the apnea event use to calculate $\text{Delta}^{\text{Mean}}{}_X$.

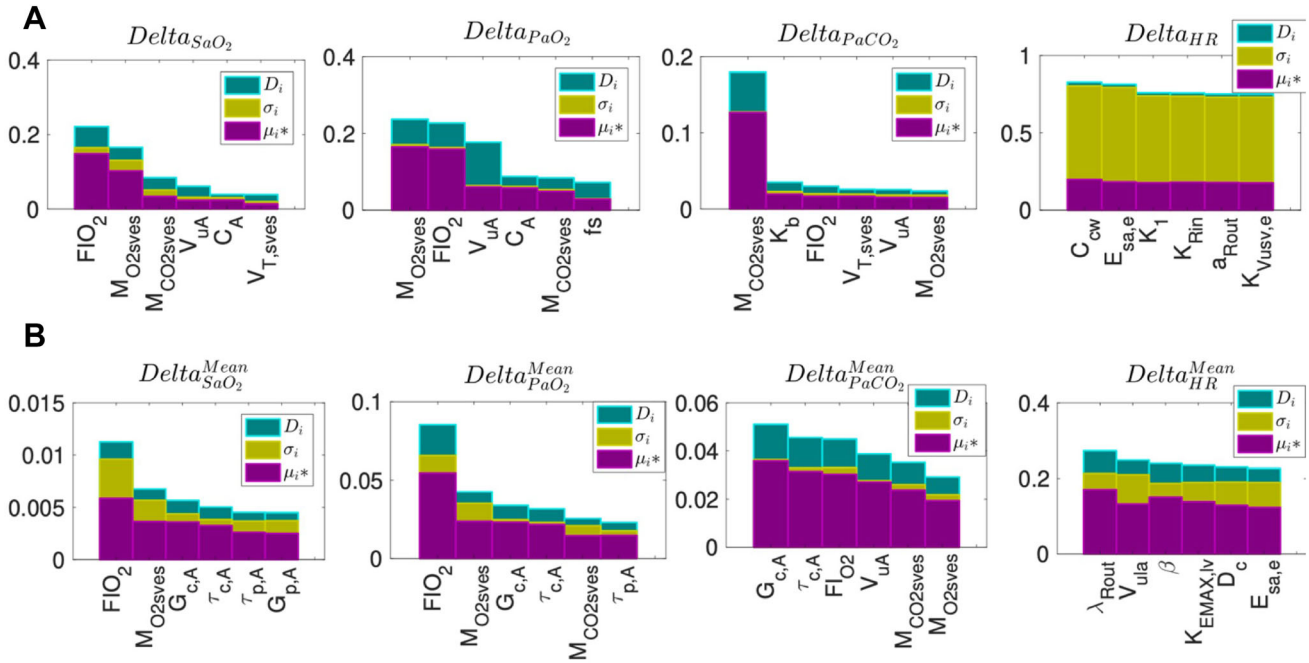

FIGURE 7. Most influential parameters of the proposed adult model obtained through the Morris screening method, using the output function Delta_X (a) and $\text{Delta}^{\text{Mean}}{}_X$ (b) , with $X \in \{\text{SaO}_2, \text{PaO}_2, \text{PaCO}_2, \text{HR}\}$. Green bars: Morris distance D_i. For each parameter, the absolute mean μ_i (purple bar) and the standard deviation σ_i (yellow bars) of the elementary effects are also displayed. Descriptions of each parameter are given in supplementary material.

apnea. Indeed, significant heart rate modifications are often observed after the apnea period. Concerning $\text{Delta}^{\text{Mean}}{}_{\text{HR}}$, the most important parameters are a sigmoid parameter of the sympathetic regulation mechanisms of the systemic resistance (λ_{Rout}), the unstressed volume of the left atrium (V_{ula}), a parameter characterizing P_{mus} during expiration (β), the gain of sympathetic regulation of the end-systolic elastance in the left ventricle ($K_{\text{EMAX,lv}}$), delay from the systemic arteries to the central chemosensitive area (D_{c}) and the elastance of the extrathoracic systemic arteries ($E_{\text{sa,e}}$).

From the results shown in Fig. 7, the most important parameters are related to the following mechanisms in the physiology: (i) the fraction of oxygen in inspired air (FIO_2), (ii) metabolic rates (M_{O2sves}, M_{CO2sves}), (iii) chemoreflex (gains: $G_{\text{c,A}}$, $G_{\text{p,A}}$; time constants: $\tau_{\text{c},A}$ and $\tau_{\text{p,A}}$), (iv) respiratory mechanics (V_{uA}, C_A). Using the quantitative approach described in the methodology, FIO_2, M_{O2sves} and $G_{\text{c,A}}$ were highlighted as the most sensitive parameters overall for Delta_X and $\text{Delta}^{\text{Mean}}{}_X$.

Local Sensitivity Analysis

Local sensitivity analyses were performed on alveoli volume, SaO_2, PaO_2, $PaCO_2$ and HR with the most influential parameters overall (FIO_2, M_{O2sves} and $G_{\text{c,A}}$). This analysis consists of an exploration of the parameter domain with a uniform distribution within predefined boundaries (see Fig 8).

Local sensitivity analyses concerning FIO_2 and M_{O2sves} (Figs 8a and 8b, respectively) show similar dynamics but with inversely proportional effects. A lower

FIO_2 (or a higher M_{O2sves}) evokes an increase of respiratory ventilation, through the peripheral chemoreflex (Figure 4.2 of the supplementary materials), and decreases directly the baseline of the PaO_2 and SaO_2. When the apnea starts from a lower PaO_2, the steeper decline in SaO_2 reflects the change of slope of the oxygen dissociation curve. A higher M_{O2sves} produces a more profound desaturation because of the lack of airflow to the lungs during the apnea. The metabolism is the only mechanism changing the amounts of O_2 and CO_2 in our model. Although heart rate does not variate significantly during apnea, a lower FIO_2 or a higher M_{O2sves} induce oscillations of HR because the increased activity of the pulmonary stretch receptors due to the important changes in ventilation that amplifies the RSA (Figure 4.2 of the supplementary materials).

Concerning $G_{\text{c,A}}$ (Fig. 8c), the amplitude of the simulated variables are not significantly modified, but a marked phase shift can be observed. During obstructive apnea, the chemoreflex has no relevant influence, because the closed upper airways block the air flow to the lungs. A higher $G_{\text{c,A}}$ produces a faster increase of the alveolar volume after apnea, increasing the activity of the pulmonary stretch receptors, amplifying the RSA, as mentioned in the description of the pulmonary stretch receptors sub-model. When $G_{\text{c,A}}$ amplitude is too important, an overcompensation phenomenon can be observed after the apnea, with a first increase of lung volume, followed by a compensating reduction of lung volume that can generate a subsequent apnea.

FIGURE 8. Local sensitivity analysis of: a the fraction of oxygen of inspired air (FIO_2); b the metabolic rate of oxygen consumption (M_{O2sves}) and c the central chemoreflex gain for the amplitude of the respiratory muscles ($G_{\text{c,A}}$) of the adult model during an obstructive apnea. ▶

DISCUSSION

This paper proposes a novel integrated model of cardio-respiratory interactions, for the analysis of acute responses to OSA events. Heterogeneous sub-models were coupled to represent original representations of: (i) mechanisms involved in RSA, (ii) interactions between discrete cardiac electrical conduction system and lumped-parameter cardiorespiratory models, (iii) integration of metabolism in circulatory model and (iv) an analytic representation of the respiration pattern adapted to adults.

Sensitivity analysis methods were applied to evaluate the relative significance of model parameters on SaO_2, PaO_2, $PaCO_2$, and HR before, during and after an OSA event. The most sensitive parameters highlighted in Fig. 7 are related to the following mechanisms in the physiology:

- *Fraction of oxygen in inspired air (FIO_2)* A lower FIO_2 decreases the baseline value of the PaO_2 and SaO_2 (Fig. 8a), and produces a steeper decline of SaO_2 during the apnea, due to the form of the oxygen dissociation curve. Among all sensitive parameters, only a few can be easily controlled in a clinical setup as a therapy target, and FIO_2 is one of them. This agrees with the use of oxygen therapy as a treatment of sleep apnea,[12,23] where the percentage of inspired oxygen is increased using supplemental oxygen.
- *Metabolic oxygen consumption and CO_2 production (M_{O2sves}, M_{CO2sves})* During apnea, the lack of ventilation significantly reduces or stop the flow of O_2 and CO_2 between the lungs and the environment, and the chemoreflex cannot control the

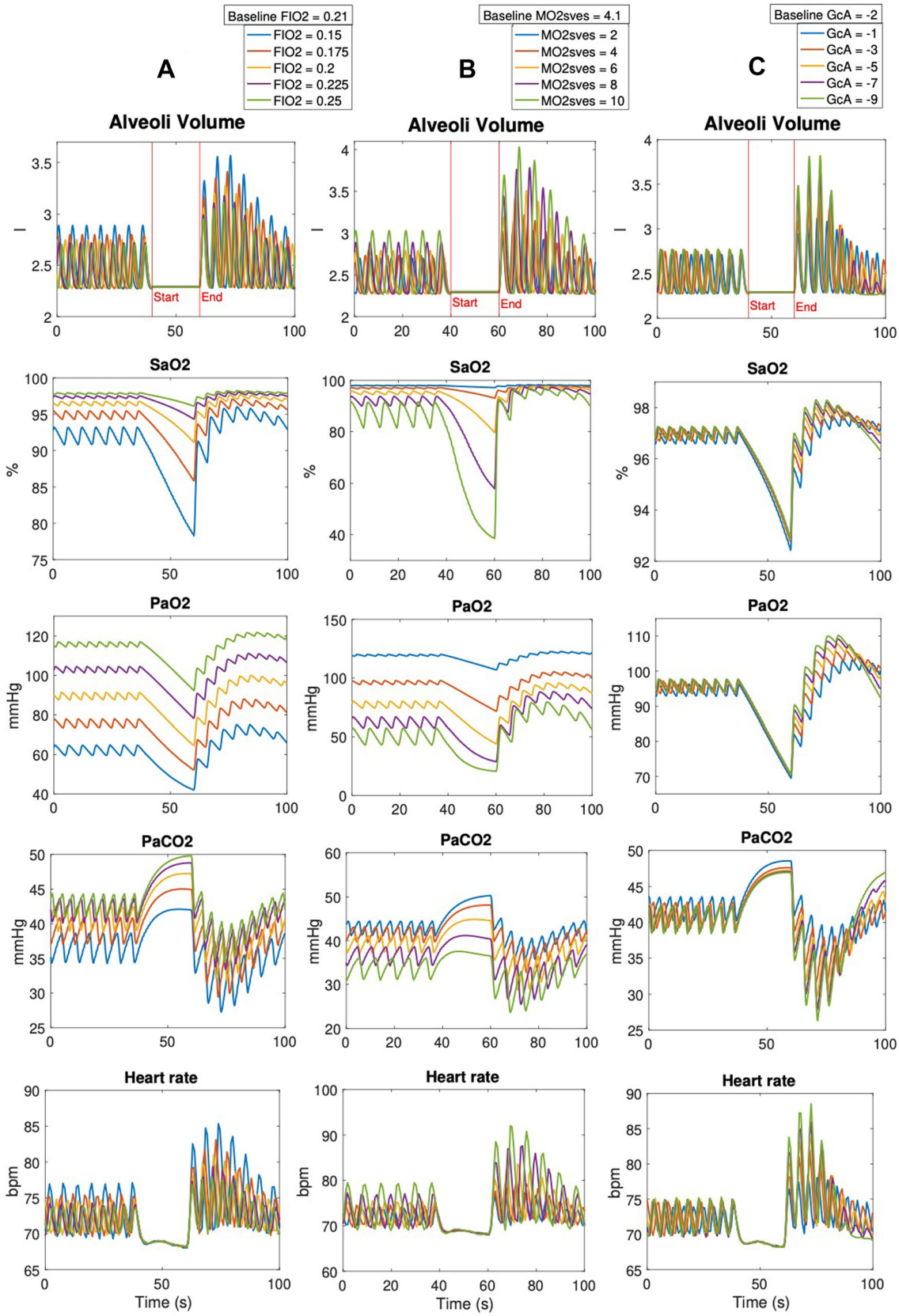
A
Baseline FIO2 = 0.21
FIO2 = 0.15
FIO2 = 0.175
FIO2 = 0.2
FIO2 = 0.225
FIO2 = 0.25
B
Baseline MO2sves = 4.1
MO2sves = 2
MO2sves = 4
MO2sves = 6
MO2sves = 8
MO2sves = 10
C
Baseline GcA = -2
GcA = -1
GcA = -3
GcA = -5
GcA = -7
GcA = -9
Alveoli Volume
Start
End
SaO2
%
PaO2
mmHg
PaCO2
mmHg
Heart rate
bpm
Time (s)

respiratory mechanical drive. Hence, only M_{O2sves} and $M_{CO2sves}$ can affect the oxygen desaturation and $PaCO_2$ modifications during apnea. A higher M_{O2sves} (Fig. 8b) leads to a deeper desaturation during an apnea, while a higher $M_{CO2sves}$ induces a faster increase of $PaCO_2$, confirming the essential role of metabolism in the acceleration of the desaturation during apneas.[21,37]

- *Chemoreflex (gains: $G_{c,A}$, $G_{p,A}$; time constants: $\tau_{c,A}$ and $\tau_{p,A}$)* During obstructive apnea, the respiratory flow is completely stopped and the chemoreflex has no influence on respiration. After the apnea, hypoxia, and hypercapnia activate the chemoreflex, and the respiration amplitude increases in order to restore O_2/CO_2 levels. This compensation effect depends on chemoreflex gains associated with respiratory amplitude ($G_{c,A}$ and $G_{p,A}$) and time constants ($\tau_{c,A}$ and $\tau_{p,A}$) of central and peripheral chemoreflex. Some higher values of $G_{c,A}$ or $G_{p,A}$ evoke substantial recovery of O_2/CO_2 partial pressures to their baseline value (Fig. 8c). When these gains are too high, an overcompensation phenomenon can be observed after the apnea, with a first significant increase of lung volume followed by a compensating reduction that can induce subsequent apnea. This confirms the increased chemoreflex sensitivity in obstructive sleep apneas.[25,40]
- *Respiratory mechanics (unstressed volume of air in the alveoli V_{uA} and lung compliance C_A)*Modifications of the lung unstressed volume (V_{uA}) lead to significant variations of functional residual capacity (FRC).[17] The FRC is the reserve of air that is used during an apnea and a higher reserve leads to a lower desaturation. Similarly, the lung compliance C_A reflects the lung's ability to stretch and expand. A high compliance value is associated with an increase in FRC.[17] The sensitivity of these parameters is in accordance with the role of ventilation therapies in OSA (continuous positive pressure [CPAP], expiratory positive airway pressure,…), which aim to increase functional residual capacity.[1,14]

During apnea, no parameter stands out in the sensitivity analysis of heart rate because HR baseline does not change strongly in model simulations during apnea. Moreover, in our model, RSA disappears during the OSA event because of the lack of lung volume variation.

Overall, the obtained results provide new insights into the underlying mechanisms of OSA, with a potential future impact on the development of novel monitoring and therapeutic strategies. The most influent parameters, obtained from the sensitivity analysis, corroborate the relevance of main treatments in adult apnea (CPAP, positive end-expiratory pressure [PEEP], oxygen therapy). For instance, monitoring of lung volume and compliance is recognized of primary importance for diagnosing the lung condition and setting ventilator parameters[20]. The stability of the negative feedback chemoreflex control system could also be measured by the loop gain method in order to provide a decision criteria to use CPAP or oxygen therapy in OSA patients[44]. Moreover, the end-tidal CO_2 concentration could be monitored using a microstream capnometer to analyze OSA severity[43].

The proposed model has also a number of potential applications within a "virtual patient" perspective. A first concrete application would be the assistance to the design of novel diagnostic or therapeutic tools. In fact, in health applications, the integration of a model-based representation could be used to conduct virtual physiological experiments and to optimize the configuration of therapeutic devices before preclinical testing phases. For example, in the context of sleep apnea, closed-loop ventilation (changing the pressure in the open airways P_{ao} of the respiratory system) or closedloop oxygen therapy[35] (adapting FIO_2) could be firstly analyzed with such a model, allowing for a better definition of the clinical evaluation phase. Previous works of our team has already shown the benefits of using such a model-based design approach for the design and optimization of a medical device.[34] Another application is to provide a virtual patient representation to improve the therapy planning by evaluating hypotheses or configuration scenarios of the system. The definition of a digital patient requires the determination of patient-specific model parameters. Results from the proposed sensitivity analysis are an essential step for dimensionality reduction, as a first step towards patient-specific parameter identification.[27,30]

The proposed model presents some limitations, mainly related to physiological mechanisms that have not been represented. For instance, the model does not include long-term control mechanisms, thermoregulation, or an adaptive metabolism module. Also, respiratory efforts against the closed upper airways, during the OSA period, have not been represented. Effects of these functions were supposed negligible on the short-term responses to sleep apnea. Although sleep stages may have an important role in the context of OSA, these mechanisms were not integrated into the proposed model and will be included in future works.

In conclusion, this paper presents the integration and analysis of a mathematical model representing cardio-respiratory interactions in the context of OSA. To our knowledge, this is the first work performing a complete sensitivity analysis to evaluate the relative significance of respiratory, cardiac, and nervous systems parameters before, during and after an obstruc-

tive apnea event. The evaluation of main physiological effects involved in SaO_2, PaO_2, $PaCO_2$, and HR responses to apnea provides results of clinical relevance concerning: (i) the fraction of oxygen in inspired air, (ii) metabolic rates, (iii) chemoreflex parameters and (iv) respiratory mechanics parameters. These significant physiological variables are highly involved in the main therapies of adult apnea (CPAP, PEEP, oxygen therapy). Finally, results concerning the relative significance of the model parameters provide valuable information for the application of such an integrated model for the analysis of OSA and suggest a convenient set of parameters to be identified in a subject-specific manner, in future works.

SUPPLEMENTARY INFORMATION

The online version contains supplementary material available at https://doi.org/10.1007/s10439-021-02828-6.

ACKNOWLEDGMENTS

Results incorporated in this publication received funding from the European Union's Horizon 2020 research and innovation program under Grant Agreement No 689260 (Digi-NewB project).

REFERENCES

[1]Abbey, N. C., K. R. Cooper, and J. A. Kwentus. Benefit of nasal CPAP in obstructive sleep apnea is due to positive pharyngeal pressure. *Sleep*. 12:420–422, 1989.

[2]Al-Omar, S., V. Le Rolle, P. Pladys, N. Samson, A. Hernandez, G. Carrault, and J. P. Praud. Influence of nasal CPAP on cardiorespiratory control in healthy neonate. *J. Appl. Physiol.* 127:1370–1385, 2019.

[3]Albanese, A., L. Cheng, M. Ursino, and N. W. Chbat. An integrated mathematical model of the human cardiopulmonary system: model development. *Am. J. Physiol.* 310(7):H899–H921, 2016.

[4]Avanzolini, G., P. Barbini, F. Bernardi, G. Cevenini, and G. Gnudi. Role of the mechanical properties of tracheobronchial airways in determining the respiratory resistance time course. *Ann. Biomed. Eng*. 29:575–586, 2001. .

[5]Ben-Tal, A., and J. C. Smith. Control of breathing: Two types of delays studied in an integrated model of the respiratory system. *Respir. Physiol. Neurobiol.* 170:103–112, 2010. .

[6]Calvo, M. Analysis of the cardiovascular response to autonomic nervous system modulation in Brugada syndrome patients. *PhD thesis, Univ. Rennes* 1, 2018.

[7]Calvo, M., V. Le Rolle, D. Romero, N. Béhar, P. Gomis, P. Mabo, and A. I. Hernández. Modelbased analysis of the autonomic response to head-up tilt testing in Brugada syndrome. *Comput. Biol. Med.* 103:82–92, 2018. .

[8]Calvo, M., V. Le Rolle, D. Romero, N. Béhar, P. Gomis, P. Mabo, and A. I. Hernández. Recursive model identification for the analysis of the autonomic response to exercise testing in Brugada syndrome. *Artif. Intell. Med.* 97:98–104, 2019. .

[9]Cheng, L., O. Ivanova, H. H. Fan, and M. C. K. Khoo. An integrative model of respiratory and cardiovascular control in sleep-disordered breathing. *Respir. Physiol. Neurobiol.* 174:4–28, 2010.

[10]Dempsey, J. A., S. C. Veasey, B. J. Morgan, and C. P. O'Donnell. Pathophysiology of sleep apnea. *Physiol. Rev.* 90:47–112, 2010.

[11]Ellwein, L. M., S. R. Pope, A. Xie, J. Batzel, C. T. Kelley, and M. S. Olufsen. Modeling cardiovascular and respiratory dynamics in congestive heart failure. *Math. Biosci.* 241:56–74, 2013.

[12]Gottlieb, D. J., N. M. Punjabi, R. Mehra, S. R. Patel, S. F. Quan, D. C. Babineau, R. P. Tracy, M. Rueschman, R. S. Blumenthal, E. F. Lewis, D. L. Bhatt, and S. Redline. CPAP versus oxygen in obstructive sleep apnea. *N. Engl. J. Med.* 370:2276–2285, 2014.

[13]Guerrero, G., V. Le Rolle, and A. I. Hernández. Sensitivity analysis of a cardiorespiratory model for the study of sleep apnea. *Comput. Cardiol.* 1–4:2018, 2010. .

[14]Heinzer, R., D. P. White, A. Malhotra, Y. L. Lo, L. Dover, K. E. Stevenson, and A. S. Jordan. Effect of expiratory positive airway pressure on sleep disordered breathing. *Sleep*. 31:429–432, 2008.

[15]Hernández, A. I., G. Carrault, F. Mora, and A. Bardou. Model-based interpretation of cardiac beats by evolutionary algorithms: Signal and model interaction. *Artif. Intell. Med.* 26:211–235, 2002.

[16]Hernandez, A. I., V. Le Rolle, A. Defontaine, and G. Carrault. A multiformalism and multiresolution modelling environment: application to the cardiovascular system and its regulation. *Philos. Trans. R. Soc. A*. 367:4923–4940, 2009.

[17]Hopkins, E., and S. Sharma. Physiology, functional residual capacity. 2019. http://www.ncbi.nlm.nih.gov/pubmed/29763183.

[18]Iooss, B., and P. Lemaître. A review on global sensitivity analysis methods. *Oper. Res. Comput. Sci. Interfaces Ser.* 59:101–122, 2015.

[19]Jean-Louis, G., F. Zizi, C. D. Brown, G. Ogedegbe, J. S. Borer, and S. I. McFarlane. Obstructive sleep apnea and cardiovascular disease: evidence and underlying mechanisms. *Minerva Pneumol*. 48:277–293, 2009. .

[20]Kulkarni, A. S. Methods to Evaluate Airway Resistance and Lung Compliance During Mechanical Ventilation: A Comparative Study. *Int. J. Innov. Sci. Res. Technol.* 5:86, 2020.

[21]Ling, I. T., A. L. James, and D. R. Hillman. Interrelationships between Body Mass, Oxygen Desaturation, and Apnea-Hypopnea Indices in a Sleep Clinic Population. *Sleep*. 35:89–96, 2012. .

[22]Lu, K., J. W. Clark, F. H. Ghorbel, D. L. Ware, and A. Bidani. A human cardiopulmonary system model applied to the analysis of the *Valsalva maneuver*. *Am. J. Physiol. Heart Circ. Physiol.* 281:H2661–H2679, 2001.

[23]Mehta, V., T. S. Vasu, B. Phillips, and F. Chung. Obstructive sleep apnea and oxygen therapy: a systematic review of the literature and meta-analysis. *J. Clin. Sleep Med.* 9:271–279, 2013.

[24]Morris, M. D. Factorial plans for preliminary computational experiments. *Technometrics*. 33:161–174, 1991.
[25]Narkiewicz, K., P. J. H. Van De Borne, C. A. Pesek, M. E. Dyken, N. Montano, and V. K. Somers. Selective potentiation of peripheral chemoreflex sensitivity in obstructive sleep apnea. *Circulation*. 99:1183–1189, 1999.
[26]Ojeda, D., V. Le Rolle, K. Tse Ve Koon, C. Thebault, E. Donal, A. I. Hernandez, K. Tse, V. Koon, C. Thebault, E. Donal, A. I. Hernandez, and A. I. Hernández. Towards an atrioventricular delay optimization assessed by a computer model for cardiac resynchronization therapy. *Proc. SPIE - Int. Soc. Opt. Eng*. 8922:333–336, 2013.
[27]Owashi, K. P., A. Hubert, E. Galli, E. Donal, A. I. Hernández, and V. Le Rolle. Model-based estimation of left ventricular pressure and myocardial work in aortic stenosis. *PLoS ONE*. 15:24, 2020.
[28]Poets, C. F. Apnea of prematurity: What can observational studies tell us about pathophysiology? *Sleep Med*. 11:701–707, 2010.
[29]Rolak, L. A., Y. Harati, and S. Izadyar. Autonomic nervous system. *Neurol. Secrets*. 2010. https://doi.org/10.1016/B978-0-323-05712-7.00012-X.
[30]Le Rolle, V., A. Beuchee, J. P. Praud, N. Samson, P. Pladys, and A. I. Hernández. Recursive identification of an arterial baroreflex model for the evaluation of cardiovascular autonomic modulation. *Comput. Biol. Med*. 66:287–294, 2015.
[31]Le Rolle, V., A. I. Hernandez, G. Carrault, N. Samson, and J.-P. Praud. A model of ventilation used to interpret newborn lamb respiratory signals. Conf. Proc. IEEE Eng. Med. Biol. Soc. 2008:4945–4948, 2008.
[32]Le Rolle, V., A. I. Hernández, P. Y. Richard, and G. Carrault. An autonomic nervous system model applied to the analysis of orthostatic tests. *Model. Simul. Eng*. 2008: 2008.
[33]Le Rolle, V., N. Samson, J.-P. Praud, and A. I. Hernández. Mathematical modeling of respiratory system mechanics in the newborn lamb. *Acta Biotheor*. 61:91–107, 2013. .
[34]RomeroUgalde, H. M., D. Ojeda, V. Le Rolle, D. Andreu, D. Guiraud, J. L. Bonnet, C. Henry, N. Karam, A. Hagege, P. Mabo, G. Carrault, and A. I. Hernandez. Model-based design and experimental validation of control modules for neuromodulation devices. *IEEE Trans. Biomed. Eng*. 63:1551–1558, 2016.
[35]Sanchez-Morillo, D., O. Olaby, M. A. Fernandez-Granero, and A. Leon-Jimenez. Physiological closed-loop control in intelligent oxygen therapy: a review. *Comput. Methods Programs Biomed*. 146:1339–1351, 2017.
[36]Senaratna, C. V., J. L. Perret, C. J. Lodge, A. J. Lowe, B. E. Campbell, M. C. Matheson, G. S. Hamilton, and S. C. Dharmage. Prevalence of obstructive sleep apnea in the general population: a systematic review. *Sleep Med. Rev*. 34:70–81, 2017. .
[37]Sirian, R., and J. Wills. Physiology of apnoea and the benefits of preoxygenation. *Contin. Educ. Anaesthesia. Crit. Care Pain*. 9:105–108, 2009.
[38]Spencer, J. L., E. Firouztale, and R. B. Mellins. Computational expressions for blood oxygen and carbon dioxide concentrations. *Ann. Biomed. Eng*. 7:59–66, 1979.
[39]Stansbury, R. C., and P. J. Strollo. Clinical manifestations of sleep apnea. *J. Thorac. Dis*. 7:E298–E310, 2015.
[40]Trombetta, I. C., C. Maki-Nunes, E. Toschi-Dias, M.-J.N.N. Alves, M. U. P. B. Rondon, F. X. Cepeda, L. F. Drager, A. M. F. W. Braga, G. Lorenzi-Filho, and C. E. Negrao. Obstructive sleep apnea is associated with increased chemoreflex sensitivity in patients with metabolic syndrome. *Sleep*. 36:41–49, 2013.
[41]Ursino, M., and E. Magosso. Acute cardiovascular response to isocapnic hypoxia. I. A mathematical model. *Am. J. Physiol. Heart Circ. Physiol*. 279:H149–H165, 2000.
[42]Ursino, M., and E. Magosso. Acute cardiovascular response to isocapnic hypoxia. II. Model validation. *Am. J. Physiol. Heart Circ. Physiol*. 279:H166–H175, 2000.
[43]Weihu, C., Y. Jingying, H. Demin, Z. Yuhuan, and W. Jiangyong. End-tidal carbon dioxide concentration monitoring in obstructive sleep apnea patients. *Am. J. Otolaryngol*. 32:190–193, 2011.
[44]Wellman, A., A. Malhotra, A. S. Jordan, K. E. Stevenson, S. Gautam, and D. P. White. Effect of oxygen in obstructive sleep apnea: role of loop gain. *Respir. Physiol. Neurobiol*. 2008. https://doi.org/10.1016/j.resp.2008.05.019.